ELASTO-PLASTIC FINITE ELEMENT ANALYSIS OF PRYING OF TOP- AND SEAT-ANGLE CONNECTIONS

M. Komuro[1], **N. Kishi**[1] **and A. Ahmed**[2]
[1]*Department of Civil Engineering and Architecture, Muroran Institute of Technology, Muroran 050-8585 Japan, E-mail: komuro@news3.ce.muroran-it.ac.jp*
[2]*Department of Building, Civil and Environmental Engineering, Concordia University, Montreal, Quebec H3G 1M8, Canada*

Abstract

In order to precisely investigate an interaction between column flange and top angle's vertical leg and the effects including prying action of bolts on $M - \theta_r$ characteristics of top- and seat-angle connections, nonlinear finite element (FE) analyses for top- and seat-angle connections as one of the angle type connections were performed. In those analysis, contact model with small sliding option was applied between contacting pair surfaces of all connecting elements. Bolt pretension force was introduced in the initial step of analysis. Numerical results together with those estimated by using Kishi–Chen power model were compared with the experimental ones to examine those applicabilities. Parametric study was also performed by varying connection parameters, material properties of connection assemblages, and magnitude of bolt pretension. From this study, the following results are obtained: (1) proposed numerical analysis method can be applicable to estimate elasto-plastic nonlinear behavior of angle type connections; (2) pretension force of bolts has no effect on prying action at the initial and ultimate level of loading, but gives some effects a little at the intermediate loading level; (3) a prying action can be increased with decreasing the thickness of flange angle or increasing of gage distance from the angle heel to the centerline of bolt hole; and (4) the initial connection stiffness and ultimate moment capacity of the connections can be increased due to increasing of angle thickness, beam depth and bolt diameter, and decreasing of gage distance.

Keywords: prying force, FE analysis, top- and seat-angle connection, moment-rotation behavior

Introduction

It is widely known that the behavior of bolted connection is significantly influenced due to a prying action. Many researchers have attempted to investigate nature and influence of prying action on connection behavior and the supporting point for prying action of angle, etc. Fleischman (1988) and Chasten et al. (1989) had investigated the effect of prying action by tension bolts experimentally. It is confirmed by them that the interaction between top angle and column flange causes additional tension force in bolts due to prying action, which may depend on the factors such as: bending stiffnesses of bolt and top angle, and location of connecting bolts.

In this paper, in order to precisely investigate an interaction between column flange and top angle's vertical leg and the effects including bolt action on $M - \theta_r$ characteristics of top- and seat-angle connections, an elasto-plastic finite element (FE) analysis was performed by using ABAQUS code. The performance of the FE analysis was discussed by comparing with the experimental moment-rotation results conducted by Azizinamini et al. (1985) and Harper (1990). It is confirmed from the comparison that the nonlinear moment-rotation behavior of top- and seat-angle connections

M. Pandey et al. (eds), Advances in Engineering Structures, Mechanics & Construction, 289–301.

Table 1. Geometrical properties of top- and seat-angle connections.

FE model	Column section	Beam section	Top and seat angles					Bolt diameter d_b (mm)
			Angle section	l (mm)	g (mm)	r (mm)	q (mm)	
A1, FE5, FE6, A1np	W12×96	W14×38	L6×4×$^3/_8$	203	64	140	89	22
A2, FE8, A2np, FE8np	W12×96	W14×38	L6×4×$^1/_2$					
Test 3	W8×24	W8×21	L6×3½×$^3/_8$	152	51	89	70	
FE1, FE7, FE1np, FE7np	W12×96	W14×38	L6×4×$^3/_4$	203	64	140	89	
FE2, FE2np	W12×96	W14×38	L6×3½×$^3/_8$		51			
FE3, FE3np	W12×96	W14×38	L6×6×$^3/_8$		114			
FE4, FE4np	W12×96	W14×38	L6×4×$^1/_2$		63.5			19
FE9, FE9np	W12×96	W8×28	L6×4×$^3/_8$					22
FE10, FE10np	W12×96	W8×28	L6×4×$^1/_2$					
FE11, FE11np	W12×96	W8×28	L6×4×$^3/_4$					
FE12, FE12np	W12×96	W8×28	L6×3$^1/_2$×$^3/_8$		51			
FE13, FE13np	W12×96	W8×28	L6×6×$^3/_8$		114			

for large deformation region can be analyzed by using proposed FE analysis method taking pretension force of bolts, contact effects and sliding frictional effects of connecting elements into account. In addition, an applicability of Kishi–Chen power model was also verified by comparing with the experimental as well as the numerical results from FE analysis.

A parametric study was also conducted to investigate the effect of parameters on prying action and moment-rotation behavior of the connections. In this analysis, the dimensions of connection models, material properties of the connection components, and magnitude of the pretension forces surcharged to the bolts were taken as variables.

FE Analysis Method

Geometry of Connection Models

Dimensions of connection models for FE analysis are shown in Table 1 corresponding to the descriptions of column and beam section sizes, in which the connection parameters listed in Table 1 are shown in Figure 1. The other connection parameters are kept constant in all connection models and those are also shown in Figure 1. In this table, test specimens A1 and A2 were taken from the experiments of Azizinamini et al. (1985) and Test 3 was taken from Harper's thesis (1990). Specimens for numerical analysis are the same to those of test specimens A1, A2, and Test 3 and the specimens for numerical simulation in case varying some parameters of test specimen are also listed in Table 1. In those specimens 'np' means that pretension of bolts is ignored. Nominal name and geometrical dimensions for all column and beam sections considered here are determined following the AISC-LRFD specification (1994). As an example of mesh geometries of connection, a half model of A2 is shown in Figure 2. In this model, the total number of elements and nodes are 10,330 and

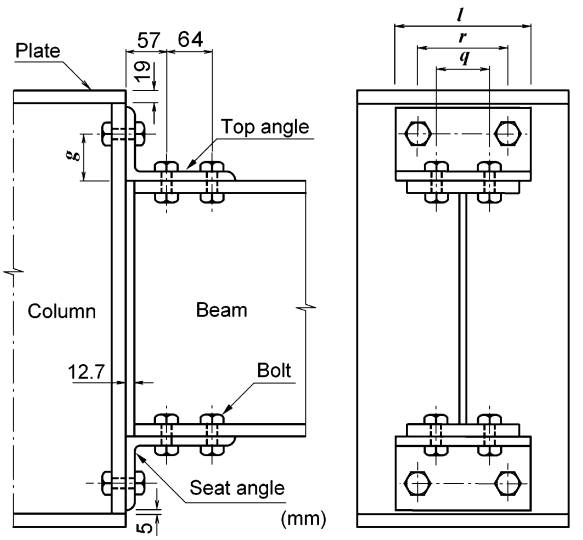

Fig. 1. Details of top- and seat-angle connection.

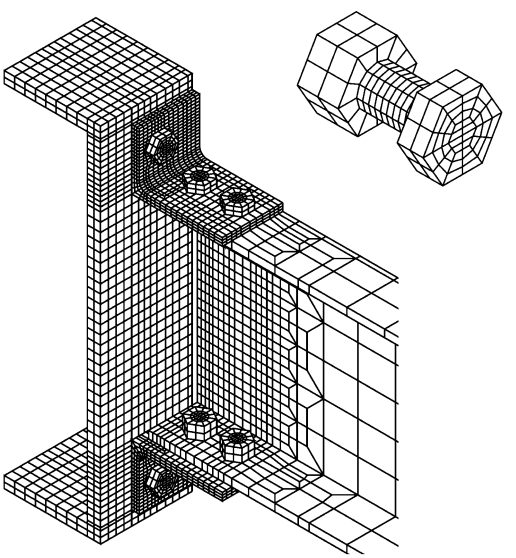

Fig. 2. Mesh pattern of FEA model A2.

17,984, respectively. All components including bolts are composed of eight node solid elements. Bolts in the mesh are divided into shank, head and nut elements to consider their individual effects on connection behavior. The diameter of bolt hole is set to be 1.6 mm (1/16 in) larger than that of bolt in accordance with Azizinamini et al.'s (1985) test data.

Mechanical Properties

Mechanical properties of angles and bolts used in numerical analysis are listed in Table 2. The mechanical properties of angles for all connection models except models FE7 and FE7np are the

Table 2. Mechanical properties used in FE analysis for top- and seat-angle connections.

Test or FEA model	Top and seat angles		Bolt	
	Yield stress σ_y (MPa)	Ultimate strength σ_u (MPa)	Yield stress $\sigma_{y,b}$ (MPa)	Ultimate strength $\sigma_{u,b}$ (MPa)
Test 3	297	517	635	830
A1, A2, FE1~FE6, FE9~FE13, A1np, A2np,FE1np~FE4np, FE9np~FE13np	365	550	635	830
FE7, FE7np	250	400		
FE8, FE8np	365	550	830	1,035

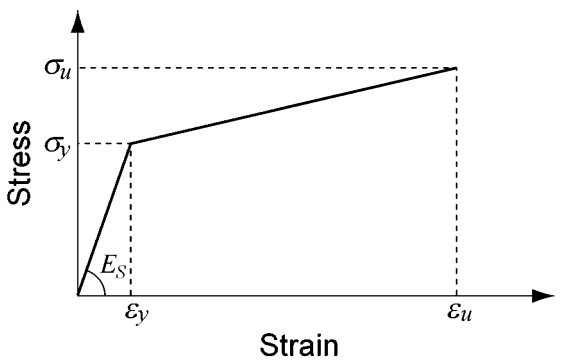

Fig. 3. Stress-strain relationship for steel used in this analysis.

same among them, which are taken from the test data for experiments conducted by Azizinamini et al. (1985). To investigate the effects of mechanical properties of angle on prying action, those for models FE7 and FE7np are assumed to be equal to the nominal values of A36 steel. Yield stress and ultimate strength of steel for beam, column and angles of all connection models are assumed to be 365 MPa and 550 MPa, respectively. Mechanical properties for bolts of all connection models except models FE8 and FE8np are assumed to be the nominal values of A325 bolts and those for models FE8 and FE8np are assumed to be equal to the nominal values of A490 bolts following the AISC-LRFD specifications because no coupon test results were reported yet. A bilinear elasto-plastic stress-strain relationship with isotropic hardening rule is assumed for all connection members taking Young's modulus of elasticity $E = 206$ GPa and Poisson's ratio $\nu = 0.3$ as shown in Figure 3. Here, ultimate strain ε_u is assumed to be 10% for bolt and 20% for another connection components.

Analytical Procedure

Numerical analyses of all connection models were performed using ABAQUS standards (1998), which was developed based on Finite Element Methodology. All components for each connection were modeled using first-order eight-node C3D8 solid elements. Here, pretension forces of bolts for all connection models except models A1np, A2np, FE1np through FE4np, FE7np through FE13np, FE5 and FE6 were prescribed up to 40% of the ultimate strength of bolt, and those for connection models FE5 and FE6 were prescribed up to 20% and 60%, respectively. The numerical results for

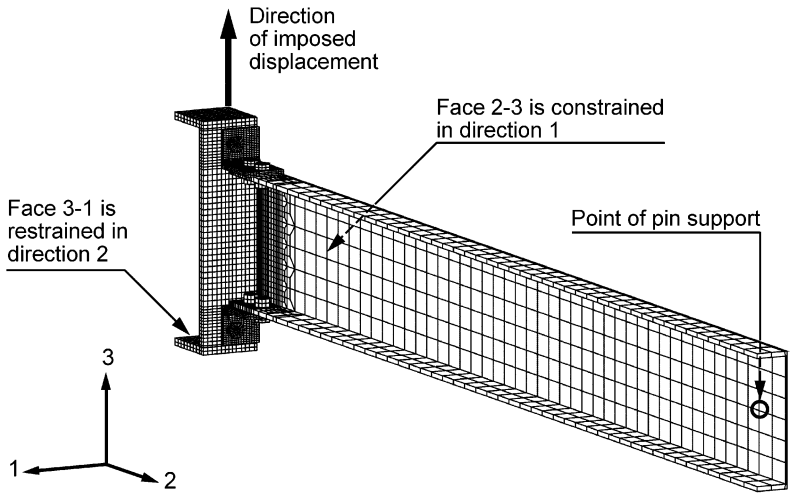

Fig. 4. Boundary conditions of FEA model of top- and seat-angle connections.

the models without pretension forces in bolts are used to estimate prying forces due to introducing pretension forces in bolts.

Numerical analysis was performed considering real experimental setup and loading method applied by Azizinamini et al. (1985), in which (1) two beams were symmetrically connected to the column flanges in a cruciform shape; (2) the ends of those beams were simply supported; and (3) the center of top plate of stub column was moved in upward direction as prescribed bending moment to be surcharged to the connection assemblages. Based on such experimental setup and considering structural symmetry, one-quarter model of connection composed of stub column, beam, top and seat angles and bolts was used for numerical analysis. Figure 4 shows a FE analysis model used for numerical analysis. The FE analyses considering pretension forces in bolts were performed in three loading steps. In the first step, a pressure equivalent to a prescribed pretension force is applied to the predefined section of bolt shank. As a result, the length of bolt shank at the pretension section changes by necessary amount to carry the prescribed load. In the second step, the prescribed load in bolt is replaced by changing the length of pretension section back into the initial length. In the third step, bending moment is introduced to the beam-to-column connection by employing vertical displacement at the middle section of plane 3–1 of the stub column (see Figure 4).

To precisely analyze the behavior of connecting members, contact model with small sliding option was applied for the contact surfaces between the vertical leg of angle and column flange, between the horizontal leg of angle and corresponding beam flange, and between the bolt and bolt hole elements. Moreover, to consider friction force occurring between sliding surfaces, Coulomb's frictional coefficient is assumed to be 0.1.

Analysis Results and Discussions

An Applicability of Proposed FE Analysis Method and Power Model

Initially, to assess an applicability of the proposed FE analysis method for simulating moment-rotation behavior of top- and seat-angle connections, numerical analyses for three connection models were performed and those numerical results together with those obtained using Kishi–Chen's three-parameter power model (1990) were compared with the experimental ones. The results of the first

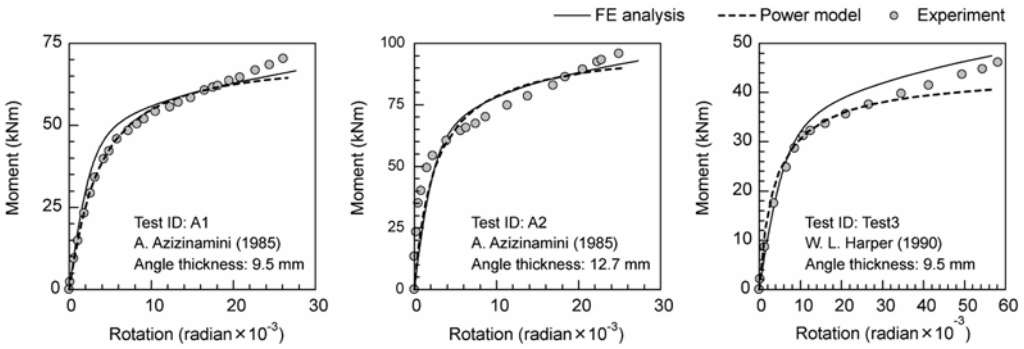

Fig. 5. Comparison of $M - \theta_r$ curves among FE analysis, power model and experiment.

two experiments (A1 and A2) reported by Azizinamini et al. (1985) and the other Test 3 reported by Harper (1990) were used for the comparisons. Following those experiments, a prescribed pretension force (40% of ultimate strength of bolt) was considered for all bolts of the connection. The comparisons of $M - \theta_r$ curves among analytical and experimental results are shown in Figure 5. It is observed that the curves obtained from FE analysis and power model prediction equation are almost similar to the experimental ones in the linear elastic and early plastic ranges. However, maximum moments from FE analysis for connection models A1 and A2, and from power model for all the three cases are smaller than those from test data. The differences among those three results in the plastic region may be caused by the following reasons:

(1) In the power model, angles are treated as perfectly elasto-plastic material and bolts are assumed to be perfectly rigid body, and the locations where plastic-hinges are formed in angles are logically fixed;
(2) There are some differences between the material properties used in FE analysis and those of test specimens.
(3) There may be experimental errors.

Even though analytical results differ a little from experimental ones, it is supposed that the proposed FE analysis method can be applied to more precisely investigate nonlinear connection behavior of top- and seat-angle connections considering pretension force introduced in bolts. In addition, it is also reasonable to conclude that the power model has a potential to predict $M - \theta_r$ curves of top- and seat-angle connections satisfactorily.

Stress-Deformation Behavior of Connection

Figure 6 shows the deformation configuration at ultimate state for model A2. From this figure, it is observed that although the horizontal maximum displacement is occurred at the heel of top angle, the vicinity of the bolt hole of top angle's vertical leg is deformed severely. Figure 7 shows the von Mises stress contour at ultimate state for model A2, in which at this time, applied connection moment is evaluated to be 103.5 kNm. From this figure, it is confirmed that the comparatively higher stresses were developed near the bolt hole and fillets of top angle. The bending moment evaluated using the reaction force developed at the beam end support can be converted into tension and compression forces in the connection, which are transferred to the column flange through the bolts fastening angles to the column flange. The bolts are elongated due to the bending-tension force applied to the

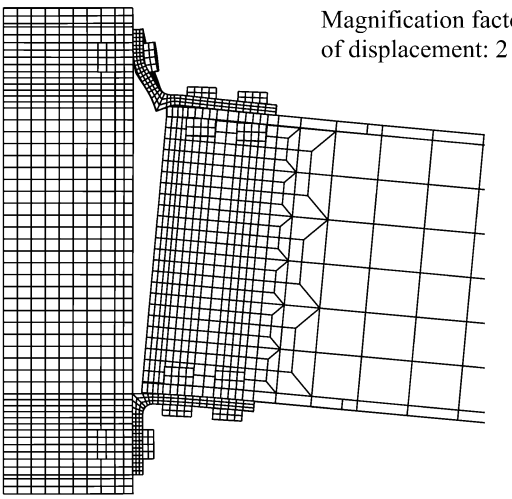

Fig. 6. Deformation configuration of connection model A2 at ultimate state.

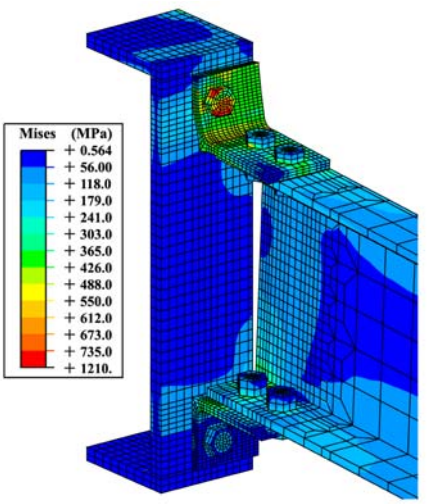

Fig. 7. Von Mises stress contour at ultimate state for model A2.

top angle, and the top angle's vertical leg behaves as a lever supported in the area from the upper portion of bolt hole through the top edge. As a result of interaction among top angle, column flange and bolts, a reaction pressure is developed in the area from the centerline of bolt hole through the top edge. To keep the forces acting in the top angle in equilibrium state, an equivalent additional tensile force corresponding to the reaction pressure is surcharged to the bolts. The reaction pressure developed on vertical leg can be substituted by a resultant, which is well known as prying force. So, tension bolts undergo not only pretension and bending-tension forces but also prying force.

Distribution of Forces in Tension Bolt

Figure 8(a) shows the distribution of internal forces in tension bolt for the case of model FE12np, in which initial pretension force introduced in bolts is ignored. The total tensile force surcharged to the

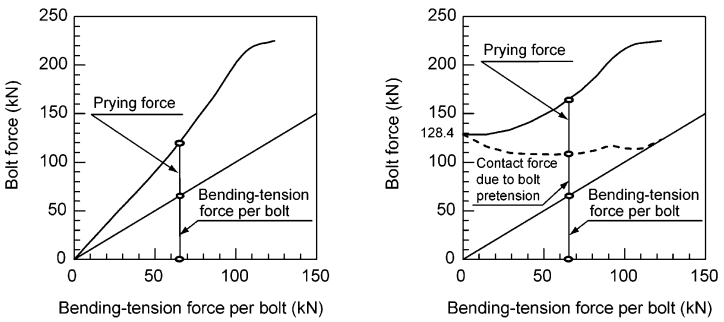

(a) Model FE12np (b) Model FE12

Fig. 8. Distribution of forces in tension bolt.

bolt for this case is evaluated as the summation of shear force applied to the top angle (hereinafter, shear force) which is equivalent to the tensile force applied to the upper flange of beam, and prying force because no pretension is applied to the bolts. From this figure, it can be observed that tensile force applied to the bolt is almost one and half time as much as shear force up to near the ultimate state. If the bending stiffness of top angle were infinite, tensile force applied to bolt would be equal to shear force applied to the angle.

It is apparent that prying force is also subjected to the tension bolts in case introducing pretension of model FE12 (Figure 8b). However, it is difficult to estimate the prying force subjected to tension bolts because bolt force consists of three components: shear force applying to top angle, contact force due to bolt pretension, and prying force. The shear force is determined as the transferred force from beam flange, whereas the other two forces can be determined as contact force that is the summation of contact force due to bolt pretension and prying force. In this study, to classify the contact force into the two forces, it is assumed that the distribution of prying force corresponding to shear force in case considering bolt pretension is similar to that for case ignoring pretension forces in bolts because it is confirmed that distribution of prying force in both cases considering with/without pretension forces in bolts is almost the same according to the results obtained from pre-analysis for investigating the influence of bolt pretension on prying action. Figure 8(b) shows the distribution of forces subjected in tension bolt of model FE12, which is the case by considering pretension forces in bolts. It is seen that three components of bolt force can be properly estimated. From this figure, it is observed that the contact force component caused by pre-tensioning of bolts is decreased nonlinearly with increasing of the shear force applied to the top angle's vertical leg.

Influence of Bolt Pretension on Prying Force and Connection Behavior

Figure 9 shows the comparisons of (a) distributions of bolt forces; (b) $M - \theta_r$ curves; and (c) initial connection stiffness among four connection models considering different levels of pretension forces in bolts. These models are A1np, FE5, A1, and FE6 for which initial pretension forces (C_0) are considered to be 0%, 20%, 40%, and 60% of the ultimate strength of bolt, respectively, and all the other properties are same among them. From Figure 9(a), it can be observed that the bolt tensile forces starting from different levels of pre-tensioning force get closer among them with increasing of bending tension force, and finally those reach at the same point. Thus, prying force near ultimate level of loading is not affected by the magnitude of pretension force. At the higher level of loading, contact force due to pre-tensioning of bolts is entirely neutralized, and only prying force is retained.

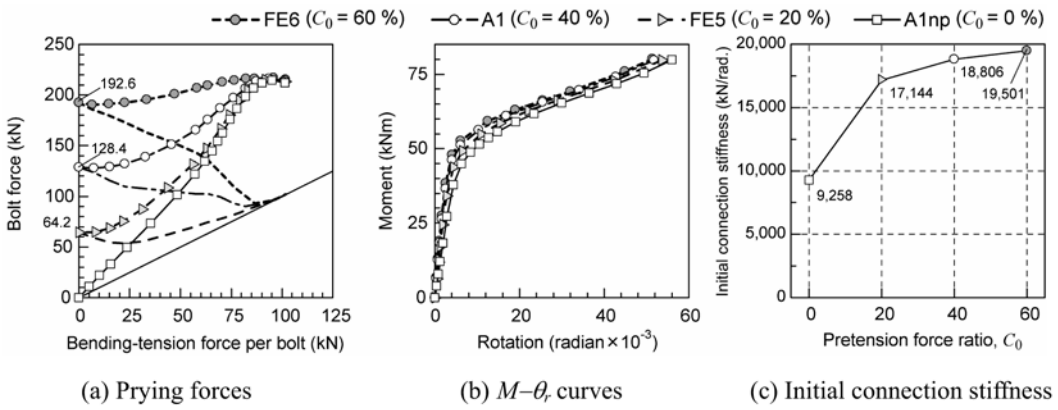

Fig. 9. Bolt pretension effect on prying force, $M - \theta_r$ curves, and initial connection stiffness.

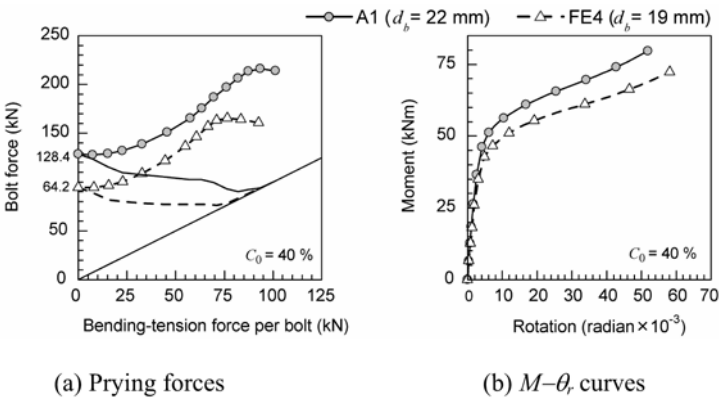

Fig. 10. Influence of bolt diameter on prying force and moment-rotation behavior.

From Figure 9(c), it can be observed that initial connection stiffness is largely increased by 85% for increasing pretension force from nil to snug-tightened level (20% of ultimate strength of bolt). Further increment of pretension forces in bolts is less effective in enhancing initial connection stiffness. When pretension force for bolt is increased from $C_0 = 20\%$ to 40 % and 60 %, initial connection stiffness is increased by 10% and 14%, respectively, with reference to the value at $C_0 = 20\%$. However, the ultimate moment capacity remains almost the same among the four cases (see Figure 9b).

Influence of Connection Parameters on Prying Force and $M - \theta_r$ Behavior

Bolt Diameter

The influence of bolt diameter on bolt force and $M - \theta_r$ curve of connection was investigated using numerical results obtained by inputting $d_b = 22$ mm and 19 mm for bolt diameter. Figure 10 shows the comparisons of distribution of prying force and $M - \theta_r$ curve of connection for the two cases. From Figure 10(a), it is observed that (1) at the beginning of loading, prying force develops very similar in both connection models; (2) but near the ultimate state, a prying force is increased when bolts with larger diameter is used.

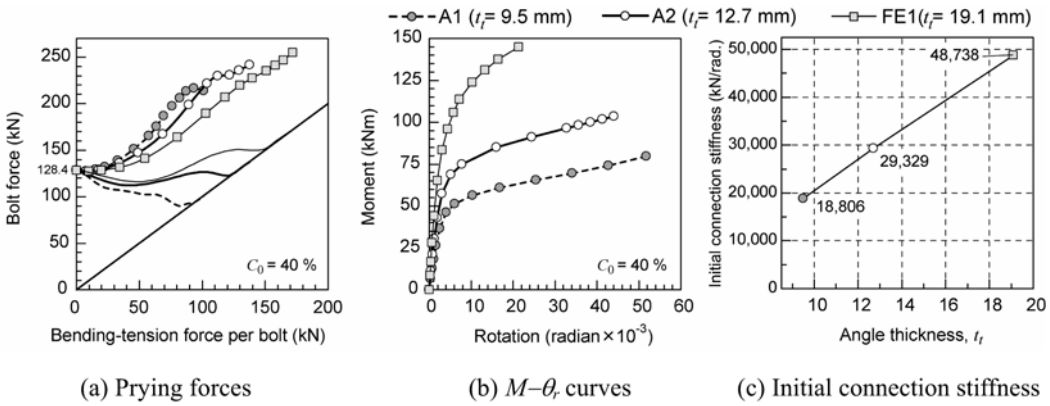

Fig. 11. Influence of flange angle thickness.

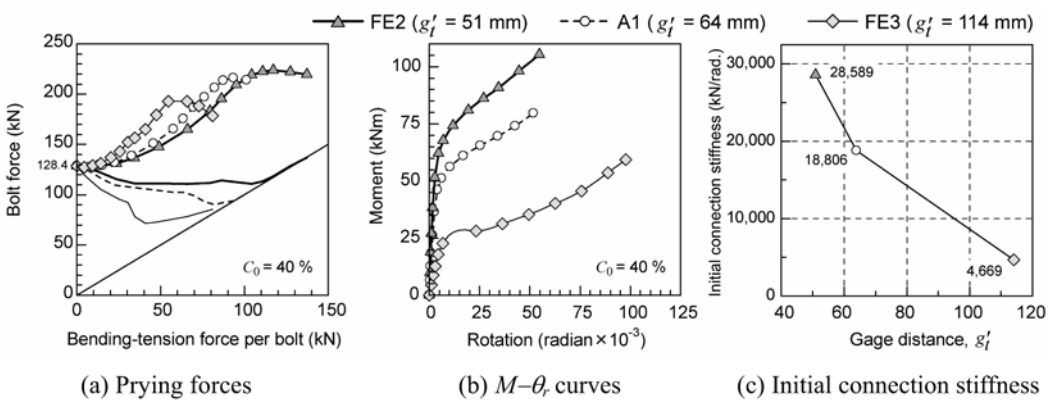

Fig. 12. Influence of gage distance from angle heel to the centerline of bolt hole.

From Figure 10(b), it is seen that even though the $M-\theta_r$ curves are almost similar to each other irrespective of the size of bolt diameter in the elastic region, the connection moment can be increased by increasing the size of bolt diameter in plastic region.

Angle Thickness

To investigate the effects of angle thickness on bolt force and $M-\theta_r$ curve of connection, numerical analysis were performed for connection model A1, A2, and FE1 in which those angle thicknesses (t_t) are assigned to be 9.5 mm, 12.7 mm, and 19.1 mm, respectively. Figure 11 shows the comparisons of bolt force, $M-\theta_r$ curve and initial connection stiffness among those three connection models. From Figure 11, it is seen that (1) the thinner the angle thickness is, the bigger the prying force is exerted and the smaller the connection moment is; (2) increasing angle thickness from 9.5 mm to 12.7 mm and 19.1 mm, ultimate connection moment is upgraded by 1.4 and 2.1 times more than that in case of 9.5 mm angle thickness, respectively; and (3) an initial connection stiffness is linearly increased corresponding to an increment of angle thickness.

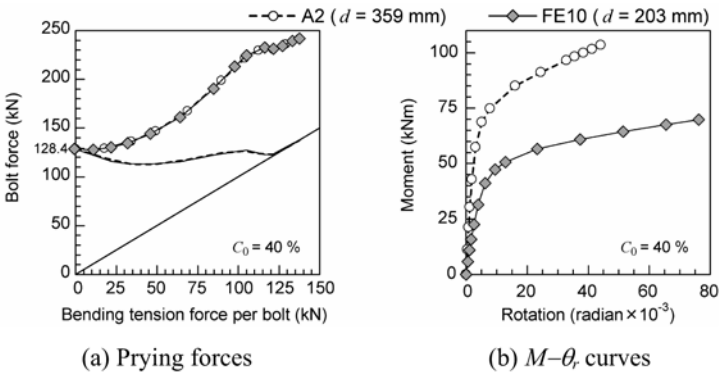

Fig. 13. Influence of beam height on prying force and moment-rotation behavior.

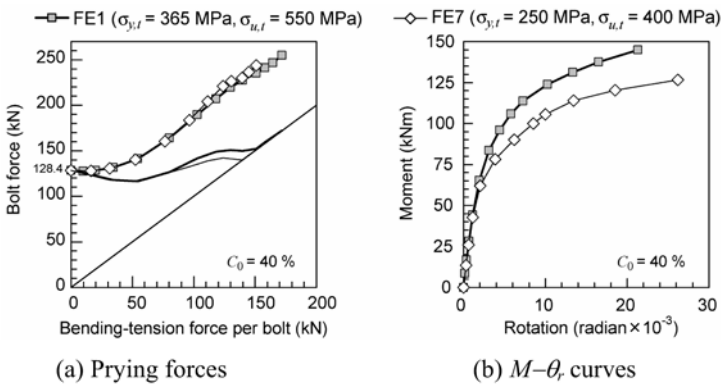

Fig. 14. Influences of mechanical properties of angle on prying force and moment-rotation behavior.

Gage Distance from Angle Heel to Centerline of Bolt Hole

Figure 12 shows the distributions of bolt force, $M - \theta_r$ curves, and initial connection stiffness in cases varying gage distance from top angle's vertical leg (g_t') as $g_t' = 51$ mm, 64 mm, and 114 mm, in which those are for models of FE1, A1, and FE3, respectively. From this figure, it is confirmed that decreasing the gage distance, (1) prying force is more increased; (2) a plastification of connection is early progressed and strain hardening effects can be expected in the large rotation area; and (3) initial connection stiffness is almost linearly increased.

Height of Beam Section

Figure 13 shows the distributions of bolt forces and $M - \theta_r$ curves in cases changing the beam height (d) as $d = 203$ mm and 359 mm, in which those are for models of A2 and FE10, respectively. From this figure, it is confirmed that the distribution of bolt force and prying force were never effected by beam height and connection moment is increased corresponding to the beam height only.

Mechanical Properties of Angle

Figure 14 shows the distributions of bolt force and $M - \theta_r$ curves in cases changing grade of angles as Azizinamini et al.'s test data and A36 steel, in which those are for models of FE1 and FE7, respectively. From this figure, it is confirmed that bolt force is not affected by mechanical properties

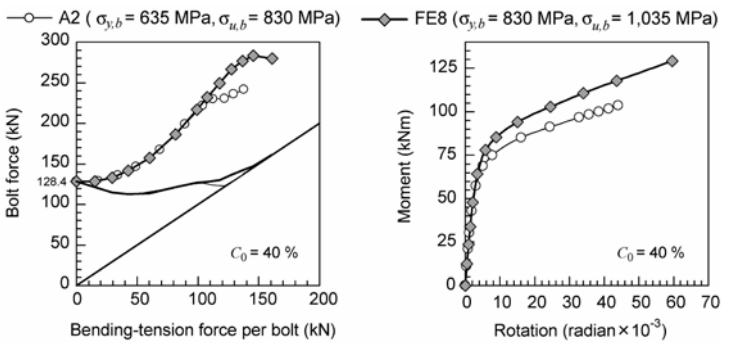

(a) Prying forces (b) M–θ_r curves

Fig. 15. Influences of mechanical properties of bolt on prying force and moment-rotation behavior.

of angle but connection moment is upgraded in the elasto-plastic region by using higher strength of angles.

Mechanical Properties of Bolt

Figure 15 shows the distributions of bolt force and $M - \theta_r$ curves, in cases changing grade of bolts as A325 and A490, in which those are for models of A2 and FE8, respectively. From this figure, it is observed that the bolt force is increased near ultimate state by taking higher grade bolts, connection moment capacity can be upgraded a little in the elasto-plastic region; and connection rotation also can be increased.

Conclusions

In this study, in order to investigate the interaction between column flange and top angle's vertical leg and these effects including bolt action on $M - \theta_r$ characteristics of top- and seat-angle connections, elasto-plastic finite element (FE) analysis was performed. Here, numerical analysis results together with the prediction by Kishi-Chen power model are compared with experimental ones to examine an applicability of the proposed analysis method and power model. In addition, to investigate the influence of connection parameters on prying force and moment-rotation behavior of top- and seat-angle connection, a parametric study was conducted by varying dimensions of connection models and magnitude of pretension force surcharged to the bolts. The following conclusions are obtained from this study:

(1) Proposed numerical analysis method can be applicable to estimate elasto-plastic nonlinear behavior of angle type connection;
(2) Power model is able to predict $M - \theta_r$ curves of the connection satisfactorily and can be applicable for nonlinear analysis of steel frames with semi-rigid connections;
(3) Pretension force of bolts has no effect on prying action at the initial and ultimate level of loading, but gives some effects a little at the intermediate loading level;
(4) A prying action can be increased with decreasing of thickness of flange angle or increasing gage distance from the angle heel to the centerline of bolt hole;
(5) Depth of beam section has no effect on prying action;
(6) Use of stiffer bolts or weaker angles in connection may increase the prying action; and

(7) Initial connection stiffness and ultimate moment capacity of the connections can be increased due to increasing of angle thickness, beam depth and bolt diameter, and decreasing of gage distance.

References

ABAQUS, 1998, *Standard User's Manual, Version 5.8*, Hibbitt Karlsson & Sorensen, Inc.

American Institute of Steel Construction (AISC), 1994, *Manual of Steel Construction, Load and Resistance Factored Design (LRFD)*, Vols I & II(2).

Azizinamini, A., Bradburn, J.H. and Radziminski, J.B., 1985, *Static and Cyclic Behavior of Semi-Rigid Steel Beam-Column Connections*, Structural Research Studies, Department of Civil Engineering, University of South Carolina, Columbia, SC.

Chasten, C.P., Fleischman, R.B., Driscoll, G.C. and Lu, L.W., 1989, Top-and-seat-angle connection and end-plate connections: Behavior and strength under monotonic and cyclic loading, *Proceedings of National Engineering Conference*, American Institute of Steel Construction, Chicago, Vol. 3, pp. 6-1–6-32.

Fleischman, R.B., 1988, Experimental and theoretical analysis of component behavior in top-and-seat-angle connections, ATLSS Project A3.1, Master's Thesis, Lehigh University, Pittsburgh, PA.

Harper, W.L., 1990, *Dynamic Response of Steel Frames with Semi-Rigid Connections*, Structural Research Studies, Department of Civil Engineering, University of South Carolina, Columbia, SC.

Kishi, N. and Chen, W.F., 1990, Moment-rotation relations of semi-rigid connections with angles, *Journal of Structural Engineering, ASCE*, 116(7), 1813–1834.